Solitary kinetic Alfvén waves in the inertial limit region

Yao Chen,[a] Zhong-yuan Li, Wei Liu, and Zhi-Dong Shi
University of Science and Technology of China, Hefei, Anhui 230026, People's Republic of China

(Received 6 July 1999; accepted 31 August 1999)

Considering the effects of hot ions and Lorentz force, a numerical study on the properties of solitary kinetic Alfvén waves (SKAWs) in the inertial limit region in the magnetosphere is presented. In contrast to the results obtained by Hasegawa and Mima [Phys. Rev. Lett. **37**, 690 (1976)], Shukla *et al.* [J. Plasma Phys. **28**, 125 (1982)], and Wu *et al.* [Phys. Plasmas **3**, 2879 (1996)], both hump and dip density Alfvénic solitons can exist in the inertial limit region ($\beta \ll 2m_e/m_i$, where β $(=2\mu_0 nT_e/B_0^2)$ is the ratio of thermal pressure to magnetic pressure). These results provide a more realistic interpretation for the SKAWs phenomena observed by the Freja satellite, in which not only SKAWs accompanied by dip density solitons, but also SKAWs accompanied by hump density solitons were found at the Earth's ionospheric altitude. © *2000 American Institute of Physics.* [S1070-664X(00)03701-0]

I. INTRODUCTION

Solitary kinetic Alfvén waves (SKAWs) may be one of the most intriguing phenomena observed by the Freja satellite. The observations indicate that there are not only SKAWs accompanied by dip density solitons, but also SKAWs accompanied by hump density solitons. Figure 1 and Fig. 2 show two examples of hump and dip density solitons,[1] respectively. The observations also show that the number of SKAWs with dip density solitons is almost the same as that of SKAWs with hump density solitons.[2]

In 1976, Hasegawa and Mima[3] analytically investigated solitons formed by the kinetic Alfvén wave (KAW) in the kinetic limit region ($2m_e/m_i \ll \beta < 1$) and found a sub-Alfvénic soliton with a density hump of arbitrary amplitude. Considering parallel ion inertia and current density, Yu and Shukla[4] studied the same problem. They suggested that localized finite-amplitude Alfvén waves with a density hump could exist. By extending similar studies to the inertial limit, Shukla[5] and Kalita[6] found a new kind of super-Alfvénic soliton with a density dip in the inertial limit region. Wu *et al.*[1] studied SKAWs in different regions, including the kinetic limit region, the transition region ($\beta \approx 2m_e/m_i$) and the inertial limit region ($\beta \ll 2m_e/m_i$). Their work indicated that hump density solitons could not exist in the inertial limit region. To explain the presence of hump density solitons observed by the Freja satellite, Wu *et al.*[1] proposed that there is a transition region dominated by oxygen plasma, in which SKAWs, accompanied by both dip and hump density solitons, are possible; Wang *et al.*[2] suggested that they had found hump density solitons in the inertial limit region. As will be shown in the following text, we contend that both their interpretations are unreasonable.

The typical altitude of the Freja satellite is 1700 km. According to the typical plasma parameters in the environments of the Freja satellite, the electron temperature is around 1 eV, the magnetic field is about 0.2–0.3 Gauss, and the particle density is $10^3 - 10^5\ \mathrm{cm}^{-3}$. So the parameter α $(=\beta m_i/m_e)$ varies between 10^{-1} and 10^{-3} in hydrogen plasma. We note that only when the oxygen component exceeds 60% can α reach 2 (the transition region). Therefore, in comparison to the chance of SKAWs encountering the inertial limit region, the chance of them encountering the transition region is too small to account for the same number of dip and hump Alfvénic solitons observed by the Freja satellite. And Wang *et al.*[2] did not eliminate the singularity of the Sagdeev potential, which was avoided by Wu *et al.*[1] In this paper, after considering the effects of hot ions, and by adding a Lorentz force into the model and thus avoiding the singularity of the Sagdeev potential, we find that hump density solitons can indeed exist in the inertial limit region.

In Sec. II and Sec. III, our magnetohydrodynamic (MHD) model and numerical method are presented, respectively. In Sec. IV, we analyze the numerical results and draw conclusions. Finally, discussions concerning future studies are given in Sec. V.

II. GOVERNING EQUATIONS

Under the assumption of low β, we can express the electric field as[6]

$$E_\perp = -\nabla\phi, \quad E_z = -\nabla\varphi, \tag{1}$$

producing an incompressible magnetic field. $E_\perp(E_z)$ is the component of the electric field perpendicular to (along) the direction of the background magnetic field $\mathbf{B}=B_0\hat{\mathbf{e}}_z$. Considering homogeneous plasma with hot ions and hot electrons, adding the Lorentz force term into the ion parallel momentum equation, the MHD equations are cast in the form

$$\frac{\partial n_e}{\partial t} + \frac{\partial (V_{ez})}{\partial t} = 0, \tag{2}$$

$$\frac{\partial \varphi}{\partial z} - \frac{Te}{e}\frac{\partial (\ln n_e)}{\partial z} = \frac{m_e}{e}\left(\frac{\partial V_{ez}}{\partial t} + V_{ez}\frac{\partial V_{ez}}{\partial z}\right), \tag{3}$$

[a]Electronic mail: chy@mail.ustc.edu.cn

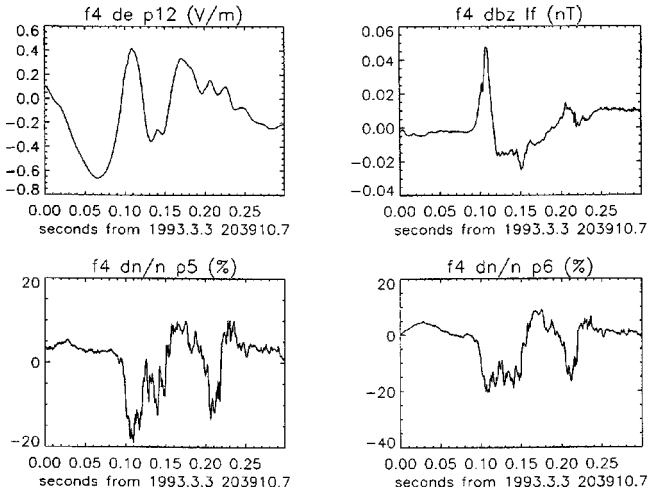

FIG. 1. The example of the SKAWs accompanied by a density dip soliton from the data of the Freja satellite on 3 March 1993.

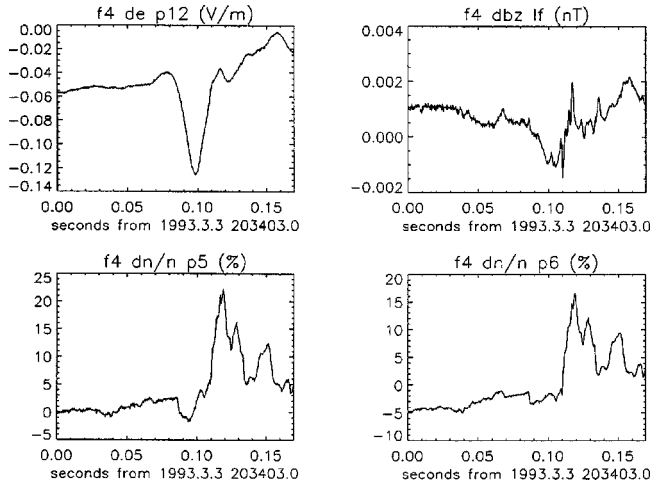

FIG. 2. The example of the SKAWs accompanied by a density hump soliton from the data of the Freja satellite on 3 March 1993.

$$\frac{\partial n_i}{\partial t}+\frac{\partial (n_i V_{ix})}{\partial x}+\frac{\partial (n_i V_{iz})}{\partial z}=0, \tag{4}$$

$$\frac{\partial \varphi}{\partial z}+\frac{m_i}{e}\left(\frac{\partial V_{iz}}{\partial t}+V_{ix}\frac{\partial V_{iz}}{\partial z}+V_{iz}\frac{\partial V_{iz}}{\partial z}\right)-V_{ix}B_y+\frac{T_i}{e}\frac{\partial (\ln n_i)}{\partial z}=0, \tag{5}$$

$$\frac{\partial B_y}{\partial x}=\mu_0 e(n_i V_{iz}-n_e V_{ez}), \tag{6}$$

$$\frac{\partial B_y}{\partial t}=\frac{\partial^2(\phi-\varphi)}{\partial x \partial z}, \tag{7}$$

$$n_e=n_i=n, \tag{8}$$

$$V_{ix}=-\frac{m_i}{eB_0^2}\frac{\partial^2 \phi}{\partial t \partial x}, \tag{9}$$

where $m_e(m_i)$, $n_e(n_i)$, $T_e(T_i)$, and $V_{ez}(V_{iz})$ are the electron (ion) mass, density, temperature, and parallel bulk velocity, respectively; J_z is the parallel current density. In order of their appearance, Eqs. (2)–(9) include electron mass continuity, electron parallel momentum, ion mass continuity, ion parallel momentum, the Ampère's Law in the parallel direction, the current density in the parallel direction, the quasineutrality condition, and the ion polarization drift velocity. In the present model, we adopt the assumption of $T_e=T_i$ for simplicity. Equations (2)–(9) become dimensionless if we introduce new variables: $n/n_0\to\overline{n}$, $V/V_A\to\overline{V}$, $e\phi/T_e\to\overline{\phi}$, $e\varphi/T_e\to\overline{\varphi}$, $B_y/B_0\to\overline{B}$, and a stationary frame, $\eta=k_\perp x+k_z z-wt$. After some transformations, Eqs. (10)–(14) are obtained.

$$\frac{d\overline{n}}{d\eta}=G, \tag{10}$$

$$\frac{d\overline{B}_y}{d\overline{n}}G=-\frac{\overline{n}}{V_A}\frac{k_\perp T_e}{eB_0}MY, \tag{11}$$

$$\frac{d\overline{\varphi}}{d\overline{n}}G=\frac{G}{\overline{n}}-G\frac{M^2}{\overline{n}^3}\frac{V_A^2}{C_e^2}, \tag{12}$$

$$\frac{dY}{d\overline{n}}G=\frac{G}{k_\perp^2\rho_s^2}\left(\frac{1}{\overline{n}^2}-\frac{C_i^2}{M^2V_A^2}\right)-\frac{d\overline{\varphi}}{d\overline{n}}G\overline{n}\frac{C_i^2}{V_A^2}\frac{1}{M^2k_\perp^2\rho_s^2}+Y\overline{B}_y\frac{\overline{n}}{V_A}\frac{w_{ci}}{k_\perp}\frac{1}{M}, \tag{13}$$

$$\frac{dG}{d\overline{n}}G=\left(Y(1-M^2\overline{n})+\frac{G^2}{\overline{n}^2}-\frac{3M^2V_A^2}{C_e^2\overline{n}^4}G^2\right)\times\left(\frac{1}{\overline{n}}-\frac{M^2}{\overline{n}^3}\frac{V_A^2}{C_e^2}\right)^{-1}, \tag{14}$$

where $Y=d^2\overline{\phi}/d\eta^2$, $M=w/k_zV_A$, and $k_z(k_\perp)$ is the component of the wave vector along (perpendicular to) the direction of the background magnetic field, $V_A(=B_0/\sqrt{\mu_0 n_0 m_i})$ is the Alfvén velocity, $C_e(C_i)$ is the electron (ion) acoustic velocity, and $w_{ce}(w_{ci})$ is the electron (ion) gyrofrequency. Eqs. (10)–(14) can be written in a general form,

$$\frac{dF}{d\overline{n}}=H, \tag{15}$$

which will be used in Sec. III. For the existence of solitary wave solutions, the following criteria are required:[1] (a) $S(\overline{n})>0$ when $1<\overline{n}<N$; (b) $S(\overline{n})=0$ at $\overline{n}=1$ and $\overline{n}=N$; and (c) $d^2\overline{n}/d\eta^2=0$ at $\overline{n}=1$; $(N-1)(d^2\overline{n}/d\eta^2)<0$ at $\overline{n}=N$. Here N represents the density maximum (or minimum); $S(\overline{n})$ represents the Sagdeev potential, which is defined as $(d\overline{n}/d\eta)^2=S(\overline{n})$. For more information about the criteria, the reader can refer to Wu *et al.*[1] We will use these criteria to construct our boundary conditions and judge whether our numerical solution is a soliton.

III. BOUNDARY CONDITIONS AND NUMERICAL METHOD

As we are interested in the localized solutions, the boundary conditions at infinity are treated as $\overline{n}=1, \overline{V}_{ez}=\overline{V}_{iz}$

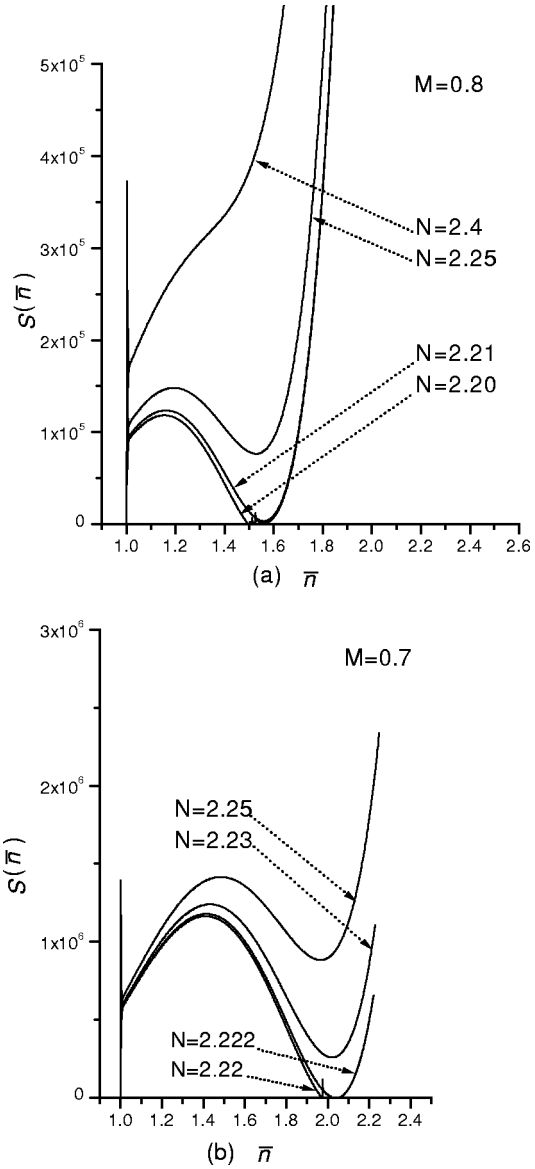

FIG. 3. The Sagdeev potential as a function of the relative particle density. The Alfvén Mach number M is set to be 0.8 (a) and 0.7 (b), respectively (sub-Alfvénic cases). Each curve corresponds to a value of N, representing a hump density soliton ($N>1$).

$=d\eta=0, \overline{B}_y=0, \eta\to\pm\infty$. In order to study the relation between the Sagdeev potential $S(\overline{n})$ and the density $\overline{n}$, we have changed the variable η to $\overline{n}$ in Eqs. (10)–(14). The computational domain is taken to be $1\leqslant\overline{n}_i\leqslant N$ ($i=1,2,...,$NUM, where NUM is the number of gird points) and discretized into uniform one-dimensional meshes with $\overline{n}_i=1$ and $\overline{n}_{\mathrm{NUM}}=N$, so the boundary conditions can be written as $Y_1=0$, $G_1=0$, $(\overline{B}_y)_1=0$, at $i=1$. We introduce the artificial fluctuation $G_2=0.01$, $Y_2=0.01$ at $i=2$. To satisfy the criteria, examples with different values of N are calculated.

We take two steps to reach the final solution. In the predictor step, we apply the direct center difference method to Eqs. (15), namely, $F^*=F_{i-1}+2H\times\Delta\overline{n}_i$, where $\Delta\overline{n}_i=\overline{n}_{i+1}-\overline{n}_i$; in the corrector step, we have $F_{i+1}=(F_{i-1}+F^*)/2$. According to their values in the environments around the Freja satellite, the plasma parameters are set to be

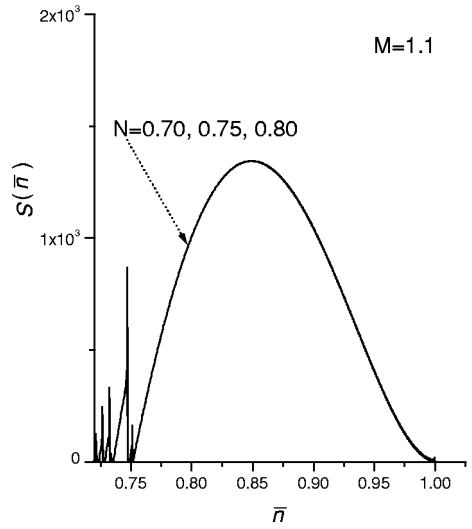

FIG. 4. The Sagdeev potential as function of the relative particle density. The Alfvén Mach number M is set to be 1.1 (super-Alfvénic cases). The three curves with different values of N, 0.70, 0.75, and 0.80 (coinciding with each other) represent dip density solitons ($N<1$).

$T_e=T_i=1$ eV, $n_0=1\times10^4\,\mathrm{cm}^{-3}$, and $B_0=0.25$ G; thus $\alpha=7.38\times10^{-3}$, $\beta=4.02\times10^{-6}$. Since $|k_\perp/k_z|\gg1$,[7] and the typical wavelength is 10^6 m,[8] we take $k_\perp=1\times10^{-5}\,\mathrm{m}^{-1}$, $k_z=1\times10^{-6}\,\mathrm{m}^{-1}$.

IV. NUMERICAL RESULTS AND CONCLUSIONS

Figure 3 to Fig. 6 show our numerical results. In every figure, we display an example with a different value of N. Figure 3 and Fig. 6 are for sub-Alfvénic ($M<1$) cases, while Fig. 4 and Fig. 5 super-Alfvénic ($M>1$). By analyzing these results, we draw conclusions as follows.

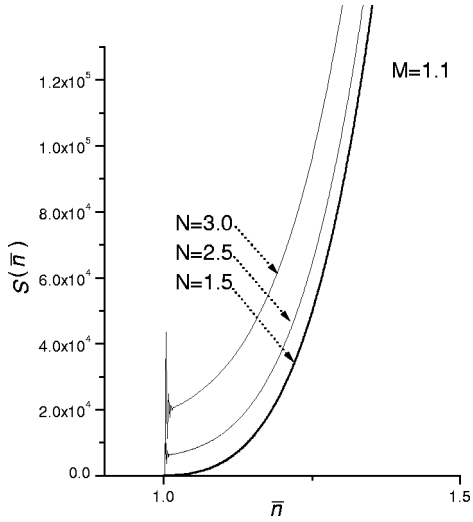

FIG. 5. When the Alfvénic Mach number $M=1.1$ and $N=1.5,2.5,3.0$, respectively, the Sagdeev potential directly approaches infinity, which indicates that in super-Alfvénic cases ($M>1$) hump density solitons ($N>1$) cannot exist.

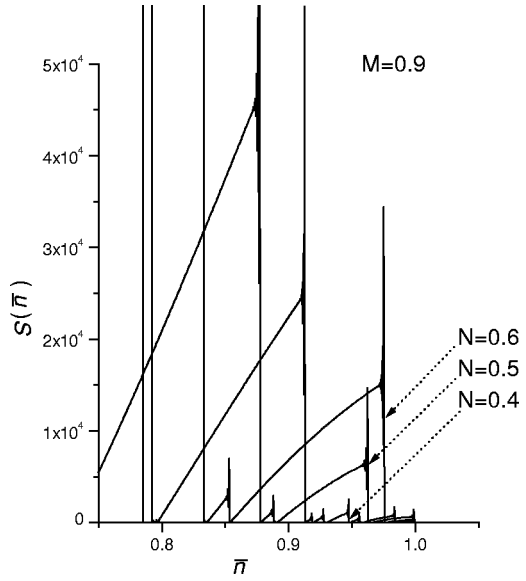

FIG. 6. The Sagdeev potential fluctuates drastically when $M<1$ and $N<1$, which suggests that in sub-Alfvénic cases dip density solitons may not exist.

(1) Hump density solitons can exist in the inertial limit region, although only when $M<1$ (see Fig. 3), which differs from the results of other authors, but agrees with the observations quite well.

(2) Hump density solitons ($N>1$) cannot exist when $M>1$ (super-Alfvénic), whereas dip density solitons can (see Fig. 4 and Fig. 5). This result coincides with that of other authors.[1,2,5,6]

(3) The density fluctuation is consistent with the observations.[8] For example, the density fluctuation can reach 25% in Fig. 4 and consequently a density cavity will be formed.

In a word, the results above can provide a more realistic interpretation for the SKAWs phenomena observed by the Freja satellite.

V. DISCUSSIONS

(1) As we know, the auroral plasma has both cold and hot components from the ionosphere or from the plasma sheet. The hot ions may have a significant effect on the soliton properties. So our consideration of the effect of hot ions is reasonable. However, for a more realistic model, kinetic theory should be employed to study this problem.

(2) As shown in Fig. 6, the solutions with $M<1$ and $N<1$ are unstable, which probably suggests that dip density solitons cannot exist in sub-Alfvénic cases in the inertial limit region.

(3) Since kinetic Alfvén waves propagate in the magnetosphere, the formation of SKAWs will be restricted by other factors, such as inhomogeneities, wave transformations, and coupling. One or more of these effects should be incorporated into the model in future work.

(4) Finally, since the soliton structure in our model is one dimensional, it cannot account for all the SKAWs phenomena observed by the Freja satellite, in which SKAWs accompanied by dipole density solitons are also observed. Therefore, a two-dimensional SKAW model would be needed, which is beyond our present scope of investigation.

ACKNOWLEDGMENT

This study is supported by the National Natural Science Foundation of China (Grants No. 49834040 and No. 49784003).

[1] D. J. Wu, G. L. Huang, D. Y. Wang, and C. G. Falthammar, Phys. Plasmas **3**, 2879 (1996).
[2] X. Y. Wang, X. Y. Wang, Z. X. Liu, and Z. Y. Li, Phys. Plasmas **5**, 4395 (1998).
[3] A. Hasegawa and K. Mima, Phys. Rev. Lett. **37**, 690 (1976).
[4] M. Y. Yu and P. K. Shukla, Phys. Fluids **21**, 1457 (1978).
[5] P. K. Shukla, H. D. Rahman, and R. P. Sharma, J. Plasma Phys. **28**, 125 (1982).
[6] M. K. Kalita and B. C. Kalita, J. Plasma Phys. **35**, 267 (1996).
[7] Z. Y. Pu and Y. N. Zhou, Science in China, Series A **12**, 1129 (1985).
[8] P. J. Louarn, E. Wanlund, T. Chust, H. de Feraudy, A. Roux, B. Holback, P. O. Dovner, A. I. Eriksson, and G. Holmgren, Geophys. Res. Lett. **21**, 1847 (1994).